Probing Colloidal Particle Aggregation by Light Scattering

Gregor Trefalt, Istvan Szilagyi, Tamas Oncsik, Amin Sadeghpour, and Michal Borkovec*

Abstract: The present article reviews recent progress in the measurement of aggregation rates in colloidal suspensions by light scattering. Time-resolved light scattering offers the possibility to measure absolute aggregation rate constants for homoaggregation as well as heteroaggregation processes. We further discuss the typical concentration dependencies of the aggregation rate constants on additives. Addition of simple salts containing monovalent counterions leads to screening of the electrostatic repulsion of the charged particles and a transition from slow to rapid aggregation. Addition of salts containing multivalent counterions may lead to a charge reversal, which results in a sequence of two instability regions. Heteroaggregation rates between oppositely charged particles decrease with increasing salt level. This decrease is caused by screening of the electrostatic attraction between these particles.

Keywords: Coagulation · Latex particles · Light scattering · Multivalent ions · Particle aggregation · Simple ions

Introduction

Aggregation in colloidal particle suspensions is a relevant process in a wide range of systems and phenomena.[1–6] In papermaking or wastewater treatment, rapid aggregation of particles must be induced to obtain the desired product or appropriate degree of water purification. Stable suspensions are needed to obtain sufficient shelf-life of consumer products or to maintain easily flowing particle slurries.

Particle aggregation can be controlled by addition of appropriate chemicals. Depending on the envisioned application, they are referred to as coagulants, flocculants, or stabilizers.[2,4,6] When aggregation is induced in an initially stable particle suspension, one obtains particle dimers first (Fig. 1).[4,7–9] Thereby, one refers to the *early stages* of the aggregation process. Since the aggregation process is irreversible, larger clusters will form as time proceeds, and one refers to *late stages*. Clusters in the late stages have irregular, fractal structures.[10,11] At lower particle
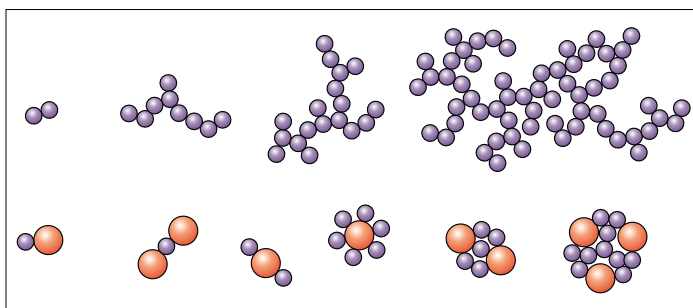

Fig. 1. Scheme of different particle aggregates. Homoaggregation (top) and heteroaggregation (bottom).

concentrations, they will eventually be influenced by gravitational forces, and sediment or cream. When the particle concentration is sufficiently high, the clusters will fill the available space, interlink, and form a colloidal gel.[12,13]

When aggregation occurs between identical (or similar) particles, one may refer to *homoaggregation*.[4,9–11] When one deals with a mixture of dissimilar particles, this fact is stressed by referring to *heteroaggregation*.[14–17] Large irregular clusters may form, but they are typically more ramified than the ones obtained in homoaggregation. More recently, small heteroaggregates of colloidal particles have been synthesized and these are referred to as *colloidal molecules*.[18–20] Such entities introduce directionality into the interactions between such particles and might eventually lead to novel functional materials.

Particle aggregation can be probed by various techniques, in particular, turbidity measurements, single particle counting, and light scattering. Widely used are turbidity measurements with a spectrophotometer.[8,21] However, the results obtained with this technique cannot be always easily interpreted. When the particle size is small, an easily measurable signal requires a rela-

tively high particle concentration, and in this situation early stages of the aggregation are difficult to probe. For larger particles, this technique can be used in a straightforward fashion, but the optical properties of the particles used must be known accurately. In single particle counting, the aggregating suspension is passed through a narrow capillary.[22,23] Thereby, the passage of each individual cluster is recorded by means of a suitable detection scheme, such as electric conductivity or light scattering. The technique offers excellent resolution, but to which extent the clusters have been disturbed by the high shear fields in the capillary cannot be easily addressed.

Time-resolved light scattering is probably the most versatile technique, which can be used in the static as well as the dynamic mode.[7,9,15,24–26] This technique operates entirely *in situ*, permits to access a wide range in particle sizes, typically from ten nanometers up to a micrometer. Moreover, the technique enables us to distinguish various types of aggregates formed. Recent progress in its utilization to probe early stages of the aggregation will be summarized here. Typical results how the aggregation rate coefficients are influenced by various salts will be equally discussed.

Correspondence: Prof. M. Borkovec
Department of Inorganic and Analytical Chemistry
University of Geneva
Sciences II
30, Quai Ernest-Ansermet
CH-1211 Geneva 4
Tel.: +41 22 379 6405
E-mail: michal.borkovec@unige.ch

Aggregation Kinetics by Light Scattering

Colloidal particles aggregate irreversibly to larger clusters, whereby the elementary step is:[4]

$$A + A \rightarrow A_2 \qquad (1)$$
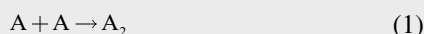
The early stages of the aggregation, when monomers and dimers dominate, can be described by the kinetic law:

$$\frac{dc_{AA}}{dt} = \frac{k_{AA}}{2} c_A^2 \qquad (2)$$

where c_A and c_{AA} are the number concentrations of monomers and dimers, t the time, and k_{AA} the aggregation rate coefficient. When only monomers and dimers dominate, one refers to the *early stages* of the aggregation.

The kinetics of colloidal aggregation can be conveniently followed by time-resolved light scattering (Fig. 2). One may use static light scattering (SLS), dynamic light scattering (DLS), and sometimes it may be advantageous to combine both. SLS measures the average scattering intensity I, while DLS gives access to the hydrodynamic radius R though the diffusion coefficient, which is obtained from the dynamics of the fluctuations of the scattered light. The doublet formation rate coefficient can be measured with SLS from the initial relative rate of change of the scattering intensities by means of Eqn. (3):[7]

$$S = \left. \frac{d \ln I}{dt} \right|_{t \to 0} = k_{AA} F_{AA}(q) = \\ k_{AA} c_0 \left(\frac{I_2(q)}{2I_1(q)} - 1 \right) \qquad (3)$$

where c_0 is the initial particle number concentration, $I_1(q)$ and $I_2(q)$ are the scattering intensities of a monomer and a dimer, respectively. Thereby, q denotes the magnitude of the scattering vector, which can be adjusted through the scattering angle. A similar expression can be obtained in the case of DLS for the initial relative rate of change of the apparent hydrodynamic radius:[7]

$$D = \left. \frac{d \ln R}{dt} \right|_{t \to 0} = k_{AA} H_{AA}(q) = \\ k_{AA} c_0 \left(1 - \frac{1}{\alpha} \right) \frac{I_2(q)}{2I_1(q)} \qquad (4)$$

where α denotes the hydrodynamic factor, which is the ratio of the diffusion coefficients of the dimer and the monomer. Since the scattering intensities can be estimated from the approximate theory of Rayleigh, Debye, Gans (RDG) of more accurate T-matrix approaches,[27–29] Eqns (3) and (4) can be used to measure the aggregation rate coefficients. This comparison is made in Fig. 3 for the aggregation of sulfate and amidine latex particles of diameters of 200 nm and 300 nm in 1 M KCl solution. One observes that RGD theory works well for smaller particles, while the T-matrix has to be used to accurately describe the angular dependence for larger particles. Under these conditions, one finds a rate coefficient of 2.7×10^{-18} m³/s for the sulfate particles and 4.0×10^{-18} m³/s for the amidine particles. The measured hydrodynamic factors are 1.46 and 1.34, which is in good agreement with the theoretical value of 1.39.

When one deals with the same (or similar) colloidal particles, one refers to *homoaggregation*. When different particles are involved, one refers to *heteroaggregation*. In early stages, the elementary step in the heteroaggregation process is:[17]

$$A + B \rightarrow AB \qquad (5)$$
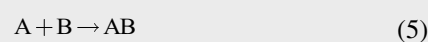
and the corresponding kinetic law is given in Eqn. (6):

$$\frac{dc_{AB}}{dt} = k_{AB} c_A c_B \qquad (6)$$

In the early stages of the aggregation of a binary particle mixture, one may have two homoaggregation processes and one heteroaggregation process occurring simultaneously. The relative rate of change of the scattering intensity has additive contributions from all three processes, namely:[17]

$$S = k_{AA} F_{AA}(q) + \\ 2k_{AB} F_{AB}(q) + k_{BB} F_{BB}(q) \qquad (7)$$

where $F_{AA}(q)$ refers to the symmetric doublets AA and represents a generalization of Eqn. (3) for a mixed system, $F_{BB}(q)$ to symmetric doublets BB, and $F_{AB}(q)$ to the analogous expression for the asymmetric doublets AB. The factors $F_{ij}(q)$ play the role of basis functions, and by means of their different angular dependencies one can distinguish the different contributions from homoaggregation and heteroaggregation within an angle-dependent measurement. For DLS, one can derive an entirely analogous expression:[17]

$$D = k_{AA} H_{AA}(q) + \\ 2k_{AB} H_{AB}(q) + k_{BB} H_{BB}(q) \qquad (8)$$

where $H_{ij}(q)$ are similar basis functions as introduced in Eqn. (7). Fig. 4 illustrates how this approach can be used to measure heteroaggregation rate constants. The initial apparent rates measured by SLS and DLS are compared. At low electrolyte concentration, only the heteroaggregation process occurs (Fig. 4a) and the measured angular dependence is solely determined by the asymmetric AB dimers. At high electrolyte concentration, all different dimers AA, AB, and BB are forming, and their different contributions are indicated (Fig. 4b). For such measurements, one can separate these different contributions, and determine the heteroaggregation rate unambiguously. From these experiments, one finds from SLS a heteroaggregation rate coefficient 7.0×10^{-18} m³/s at 10^{-4} M and 4.9×10^{-18} m³/s at 1 M, while comparable values are obtained from DLS.

Tuning Particle Aggregation by Additives

In their seminal work, Derjaguin, Landau, Verwey, and Overbeek (DLVO) recognized that particle aggregation rate is
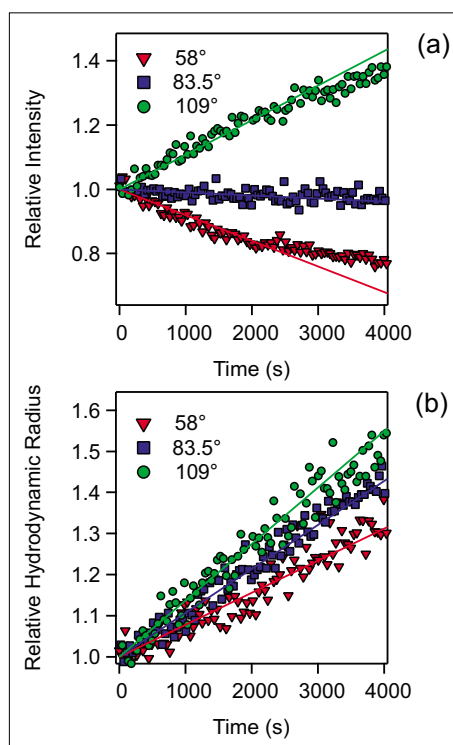
Fig. 2. Relative change in the scattering intensity and apparent hydrodynamic radius with time during particle aggregation normalized to the initial value. (a) Scattering intensity and (b) apparent hydrodynamic radius. For some scattering angles, the scattering intensity may also decrease as the aggregation proceeds.
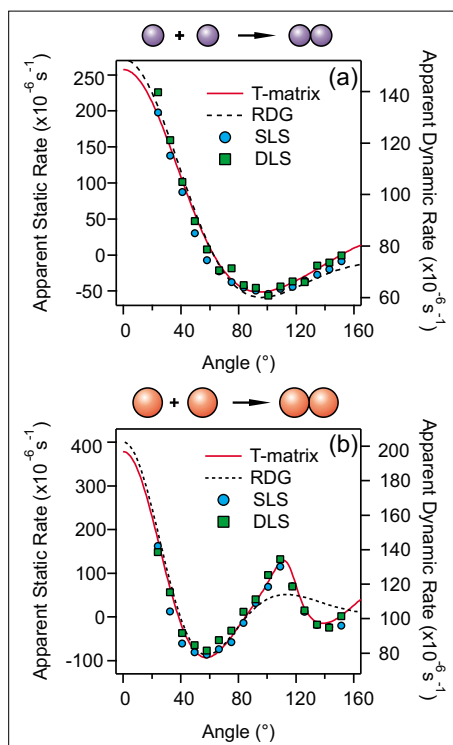
Fig. 3. Apparent aggregation rates measured by time-resolved SLS and DLS as a function of the scattering angle for homoaggregation in 1 M KCl solution and pH 4.0. Note that static and dynamic rates are proportional, and thus can be plotted within the same graph. The dashed and solid lines presents the best fits to the RDG and T-matrix model, respectively. (a) Sulfate latex particles of 200 nm in diameter and (b) amidine latex particles of 300 nm in diameter.
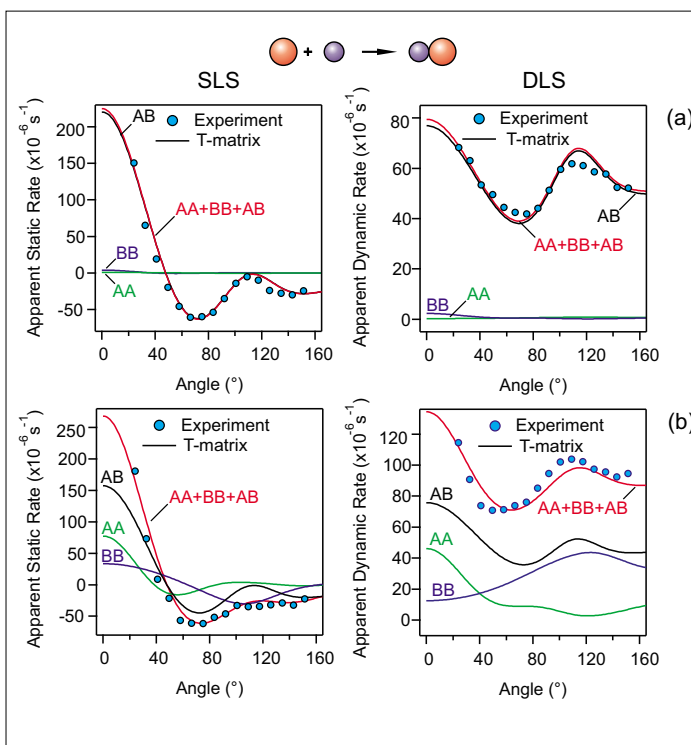

Fig. 4. Apparent aggregation rates measured by time resolved SLS (left) and DLS (right) as a function of the scattering angle for heteroaggregation in a mixture of oppositely charged sulfate (A) and amidine latex particles (B) of diameters of 200 nm and 300 nm, respectively, at a number fraction of 0.75 of the sulfate particles at pH 4.0. Lines represent the best fits to the T-matrix model whereby the contributions of the particular type of dimers AA, BB, and AB are indicated. (a) Aggregation at an electrolyte concentration of 10^{-4} M where only AB aggregates are forming, and (b) aggregation at an electrolyte concentration of 1 M where all types of aggregates form simultaneously.

determined by mutual diffusion of the two particles in their potential energy profile:[4]

$$V = V_{vdW} + V_{dl} \qquad (9)$$

with two main contributions, namely the van der Waals energy V_{vdW} and the energy due to the overlap of the electrical double layers V_{dl}.

These two contributions can nowadays be estimated with good accuracy. From the energy profile, the rate coefficient can be obtained from the known expression for diffusion controlled reactions, namely:[4,9]

$$k_{AA} = \frac{4 k_B T}{3 \eta a} \times \left[\int_{2a}^{\infty} \frac{B(r)}{r^2} \exp[V(r)/(k_B T)] \, dr \right]^{-1} \qquad (10)$$

where r is the center-to-center separation, $B(r)$ is the hydrodynamic resistance function, k_B is the Boltzmann constant, T the absolute temperature, η the solvent viscos-

ity, and a the particle radius. The above relation applies to homoaggregation of similar particles, while an analogous relation can be used to evaluate the rate coefficient for heteroaggregation. Therefore, the rate coefficients can be estimated from the solution composition and particle properties, such as their size and surface characteristics.

The DLVO theory predicts two distinct aggregation regimes. When the interaction potential is attractive, the aggregation is rapid since the approach of the particles process is mainly controlled by their mutual diffusion. In this case, one refers to the *fast aggregation regime*. When the interaction potential features an intermediate barrier, the aggregation is slow, since the particles must overcome this barrier by thermal activation. In this case, one refers to the *slow aggregation regime*. Instead of reporting rate coefficients, one often refers to the *stability ratio* defined as

$$W_{ij} = \frac{k_{fast}}{k_{ij}} \qquad (11)$$

where k_{fast} is the aggregation rate coeffi-

cient in the fast aggregation regime. Thus, a small stability ratio around unity refers to fast aggregation, while a larger value to slow aggregation.

Let us now discuss the typical dependencies of the stability ratio in some relevant situations. Fig. 5 illustrates the stability ratio for homoaggregation for negatively charged carboxylated latex particles with a diameter of 300 nm at pH 4.0 in the presence of linear aliphatic polyamines. Thereby, the number of amine groups is indicated. These polyamines are almost fully protonated, and thus represent a convenient model system to study the major effects of valence on colloidal aggregation.

The first characteristic situation occurs for counterions of low valence. At low salt concentrations, aggregation is very slow and the suspension is stable. Increasing the salt concentrations, the stability ratio decreases steeply, until the plateau at unity is reached. Increasing the salt level further, the rate coefficient remains independent of the concentration. The transition between the slow and fast aggregation regimes is referred to as the critical coagulation concentration (CCC). This transition is caused by the progressive screening of the elec-
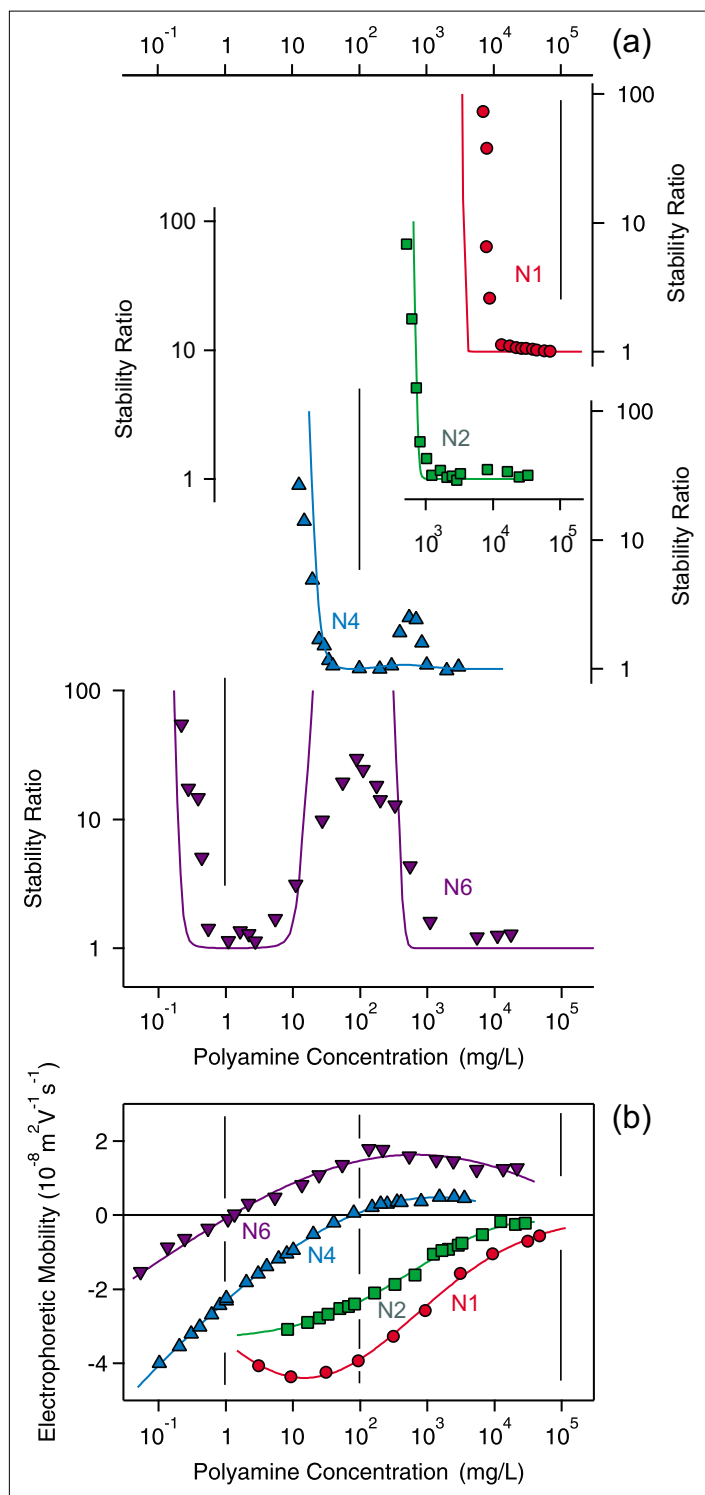
Fig. 5. Stability and charging characteristics of carboxylated latex particles of a diameter of 307 nm versus the concentration of linear aliphatic polyamines at pH 4.0. The number of amine groups is indicated. (a) Experimental stability ratios where the solid lines are predictions of DLVO theory. (b) Electrophoretic mobility results with solid lines, which serve to guide the eye only.

dicting the observed trends relatively well (Fig. 5a). The surface potentials were estimated from electrophoretic mobilities and a Hamaker constant of 4.5×10^{-21} J was used. This value is somewhat smaller than the theoretical estimate of 9.0×10^{-21} J for polystyrene,[37] probably due to roughness and retardation effects. The discrepancy for N1 is probably related to short range hydration forces, while the discrepancies near the restabilization maximum for N4 and N6 are thought to originate from surface charge heterogeneities. The experimentally observed fast aggregation rate constant is 3.1×10^{-18} m^3/s, while the DLVO theory predicts 7.1×10^{-18} m^3/s. This somewhat larger value probably originates from inaccuracies in the hydrodynamic resistance function at small separations.

Much less quantitative information is available on heteroaggregation. However, the case of two oppositely charged particles has been investigated in some detail in the presence of monovalent salt.[17] The corresponding data were measured with the multi-angle techniques described above and they are presented in Fig. 6. One observes that the corresponding stability ratio increases with increasing electrolyte concentration, but the effect is much more modest than for homoaggregation. This increase originates from the screening of the mutual electrostatic attraction of the two oppositely charged particles. The overall trend can be again well described by DLVO theory. Thereby, the surface potentials of both particles have been estimated from electrophoresis.

Conclusion

Our capabilities to measure aggregation rates in colloidal suspensions by light scattering have recently evolved substantially. By measuring the angular dependence of the light scattering signal in a time-re-
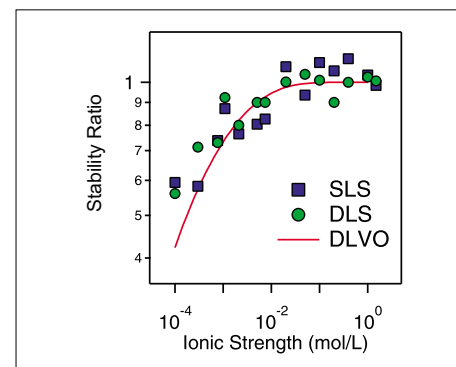

Fig. 6. Heteroaggregation rate coefficients between sulfate and amidine latex particles of diameters 277 nm and 160 nm, respectively, versus the ionic strength adjusted with KCl electrolyte at pH 4.0. The line shows calculated results with DLVO theory.

trostatic double layer interactions by the dissolved salt ions.[4,25,26]

When the valence is increased, one observes that the CCC shifts towards lower concentrations.[25,30,31] This dependence is referred to as the Schulze-Hardy rule, which states that the CCC scales as the inverse six power of the valence.[4] The data shown in Fig. 5 obey this scaling rather well. However, another characteristic feature becomes apparent for higher valence, namely the restabilization at intermediate concentrations. This restabilization is related to the charge reversal of the particles

that is induced by the adsorption of the ions of higher valence. This charge reversal can be demonstrated by electrophoresis (Fig. 5b). Similar effects involving screening and charge reversal were also observed with positively charged particles and multivalent anions.[25,30,32] However, anions appear to induce a charge reversal more easily than cations. Reversal of charge represents a key mechanism in destabilization of colloidal suspensions, and can be important in amphoteric systems, surfactants, or polyelectrolytes.[33–36]

The DLVO theory is capable of pre-

solved fashion, the absolute aggregation rates can be measured. In particular, the angular dependence permits simultaneously occurring homoaggregation as well as heteroaggregation to be distinguished. These techniques permit the study of aggregation rates in various systems. Homoaggregation of charged colloidal particles in the presence of ions of low valence is influenced by screening the electrostatic repulsion between the charged particles, and leads to a sharp transition between slow and fast aggregation. With increasing valence, this transition point shifts towards lower concentrations. However, a restabilization can be observed in the presence of multivalent ions when their valence is sufficiently high. This restabilization originates from a charge reversal induced by the adsorption of these ions. Heteroaggregation rates between oppositely charged particles decrease with increasing salt level, and this decrease can be explained by screening the electrostatic attraction between these particles. All these trends can be well rationalized by DLVO theory, even though this theory often predicts stronger dependencies than observed experimentally. With these experimental and theoretical tools, the stability of colloidal suspensions can be controlled in a much more detailed fashion than was possible so far.

[1]   D. Horn, F. Linhart, 'Retention Aids', Blackie Academic and Professional, London, **1996**.
[2]   B. Bolto, J. Gregory, *Water Res.* **2007**, *41*, 2301.
[3]   R. Nystrom, K. Backfolk, J. B. Rosenholm, K. Nurmi, *J. Colloid Interface Sci.* **2003**, *262*, 48.
[4]   W. B. Russel, D. A. Saville, W. R. Schowalter, 'Colloidal Dispersions', Cambridge University Press, Cambridge, **1989**.
[5]   P. G. de Gennes, *Nature* **2001**, *412*, 385.
[6]   M. Elimelech, J. Gregory, X. Jia, R. A. Williams, 'Particle Deposition and Aggregation: Measurement, Modeling, and Simulation', Butterworth-Heinemann Ltd., Oxford, **1995**.
[7]   H. Holthoff, S. U. Egelhaaf, M. Borkovec, P. Schurtenberger, H. Sticher, *Langmuir* **1996**, *12*, 5541.
[8]   S. H. Xu, Z. W. Sun, *Soft Matter* **2011**, *7*, 11298.
[9]   M. Kobayashi, F. Juillerat, P. Galletto, P. Bowen, M. Borkovec, *Langmuir* **2005**, *21*, 5761.
[10] P. Sandkuhler, M. Lattuada, H. Wu, J. Sefcik, M. Morbidelli, *Adv. Colloid Interface Sci.* **2005**, *113*, 65.
[11] M. Y. Lin, H. M. Lindsay, D. A. Weitz, R. C. Ball, R. Klein, P. Meakin, *Nature* **1989**, *339*, 360.
[12] T. Gisler, R. C. Ball, D. A. Weitz, *Phys. Rev. Lett.* **1999**, *82*, 1064.
[13] L. F. Rojas, R. Vavrin, C. Urban, J. Kohlbrecher, A. Stradner, F. Scheffold, P. Schurtenberger, *Faraday Discuss.* **2003**, *123*, 385.
[14] R. O. James, A. Homola, T. W. Healy, *J. Chem. Soc. Farad. Trans. I* **1977**, *73*, 1436.
[15] W. L. Yu, E. Matijevic, M. Borkovec, *Langmuir* **2002**, *18*, 7853.
[16] A. M. Puertas, A. Fernandez-Barbero, F. J. de las Nieves, *J. Chem. Phys.* **2001**, *114*, 591.
[17] W. Lin, M. Kobayashi, M. Skarba, C. Mu, P. Galletto, M. Borkovec, *Langmuir* **2006**, *22*, 1038.
[18] Y. S. Cho, G. R. Yi, J. M. Lim, S. H. Kim, V. N. Manoharan, D. J. Pine, S. M. Yang, *J. Am. Chem. Soc.* **2005**, *127*, 15968.
[19] D. J. Kraft, J. Groenewold, W. K. Kegel, *Soft Matter* **2009**, *4*, 1302.
[20] E. Duguet, A. Desert, A. Perro, S. Ravaine, *Chem. Soc. Rev.* **2011**, *40*, 941.
[21] A. Puertas, J. A. Maroto, F. J. de las Nieves, *Colloids Surf. A* **1998**, *140*, 23.
[22] H. Holthoff, A. Schmitt, A. Fernandez-Barbero, M. Borkovec, M. A. Cabrerizo-Vilchez, P. Schurtenberger, R. Hidalgo-Alvarez, *J. Colloid Interface Sci.* **1997**, *192*, 463.
[23] H. Lichtenfeld, H. Stechemesser, H. Möhwald, *J. Colloid Interface Sci.* **2004**, *276*, 97.
[24] S. H. Behrens, M. Borkovec, P. Schurtenberger, *Langmuir* **1998**, *14*, 1951.
[25] I. Szilagyi, A. Sadeghpour, M. Borkovec, *Langmuir* **2012**, *28*, 6211.
[26] C. Schneider, M. Hanisch, B. Wedel, A. Jusufi, M. Ballauff, *J. Colloid Interface Sci.* **2011**, *358*, 62.
[27] M. I. Mishchenko, D. W. Mackowski, *J. Quant. Spectrosc. Radiat. Transf.* **1996**, *55*, 683.
[28] H. Holthoff, M. Borkovec, P. Schurtenberger, *Phys. Rev. E* **1997**, *56*, 6945.
[29] P. Galletto, W. Lin, M. I. Mishchenko, M. Borkovec, *J. Chem. Phys.* **2005**, *292*, 139.
[30] A. Sadeghpour, I. Szilagyi, M. Borkovec, *Z. Phys. Chem.* **2012**, *226*, 597.
[31] I. Szilagyi, D. Rosicka, J. Hierrezuelo, M. Borkovec, *J. Colloid Interf. Sci.* **2011**, *360*, 580.
[32] P. Sinha, I. Szilagyi, F. J. M. Ruiz-Cabello, P. Maroni, M. Borkovec, *J. Phys. Chem. Lett.* **2013**, *4*, 648.
[33] M. Schudel, S. H. Behrens, H. Holthoff, R. Kretzschmar, M. Borkovec, *J. Colloid Interface Sci.* **1997**, *196*, 241.
[34] T. Hiemstra, W. H. van Riemsdijk, *Langmuir* **1999**, *15*, 8045.
[35] M. Borkovec, G. Papastavrou, *Curr. Opin. Colloid Interface Sci.* **2008**, *13*, 429.
[36] L. Liang, J. J. Morgan, *Aquat. Sci.* **1990**, *52*, 32.
[37] M. A. Bevan, D. C. Prieve, *Langmuir* **1999**, *15*, 7925.